Topology of the U12-$U6_{atac}$ snRNA complex of the minor spliceosome and binding by NTC-related protein RBM22

*Joanna Ciavarella[1,3], William Perea[3], and Nancy L. Greenbaum[1,2,3]**

[1]Ph.D. Program in Chemistry, The Graduate Center of the City University of New York, New York, NY 10016; [2]Ph.D. Program in Biochemistry, The Graduate Center of the City University of New York, New York, NY 10016; [3]Department of Chemistry, Hunter College of the City University of New York, New York, NY 10065

Supplementary Information

Nucleotide sequences for constructs.

For the bimolecular construct representing the human U12-$U6_{atac}$ snRNA complex, we used the sequence 5′- GAUGCCUUAAACUUUGAGGUAAGGAAA-3′, to represent the U12 snRNA and the sequence of, 5′- AUGAAAGGAGAGAAGGUUAGCACUCCCCUUGA-CAAGGAUGGAAGAG -3′ to represent the $U6_{atac}$ snRNA.

The unimolecular human U12-$U6_{atac}$ "chimeric" RNA had the sequence: 5′-GGUGCCUUA-AACUUCUUCGGAGGUUAGCACUCCCCUUGACAAGGAUGGAAGAG -3′.

The unimolecular *Arabidopsis* U12-$U6_{atac}$ "chimeric" RNA had the sequence: 5′-GGUGCCUUAACUACUUCGGUGGUUGGCAUCUCCUCUGACAGAGAUGGGAUUU -3′.

For the construct representing the human U2-U6 snRNA complex, we used the sequence 5′-CGCUUCUCGGCCUUUUGGCUAAGAUCUUCUCUGUAUCUGUUC-3′ to represent the U2 snRNA and 5′- GGGACUAAAAUUGGAACGUACAGAGAGAAGAUUAGCAUGGCCCCU GCGCAAGGAUGACACGAAAUUCGUGAAGCG-3′ for the U6 snRNA fragment.

For the construct representing the human U5 snRNA complex, we used the sequence 5′-GGGGATCCACATGGTTCTTGCCTTTT-3′.

Pairing and folding of RNA samples.

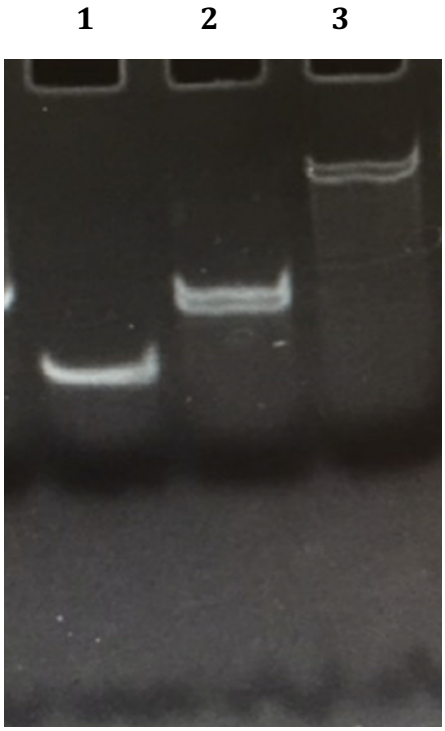

1A

Figure S-1: Pairing of equimolar quantities of individual strands of the bimolecular human U2-U6 (A) and U12-$U6_{atac}$ (B) snRNA snRNA construct were paired and incubated as described in Experimental Section. Samples were electrophoresed on a 20% non-denaturing PAGE and stained in EtBr. Shifting of the single band of the combined strands and disappearance of the bands of individual strands implies complete pairing and formation of a single conformation. **(A)** human U2-U6 snRNA (major spliceosome; sequence above, and secondary structural scheme in Fig. 1A in text) strands: Lane 1 = U2 strand; Lane 2 = U6 strand; Lane 3: paired U2 and U6 snRNA strands.

(B) human U12-U6$_{atac}$ snRNA (minor spliceosome; sequence above, and secondary structural scheme in Fig. 1B in text) strands: Lane 1 = U12 strand; Lane 2 = U6$_{atac}$ strand; Lane 3 = paired strands. See Experimental Section (in the text) for details.

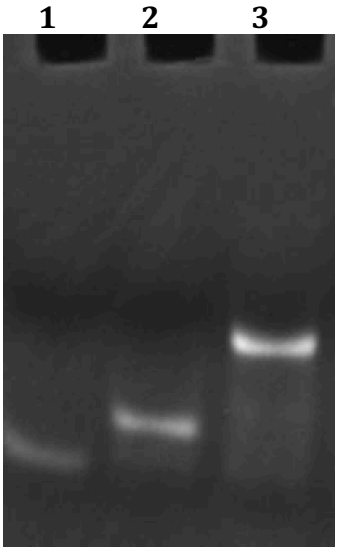

1B

Figure S-2A: Folding of bimolecular (right) and unimolecular (left) samples of the human U12-U6$_{atac}$ snRNA complex; sequences are above, and scheme of predicted folds in Fig. 1B and 2A, respectively). Both samples migrate as single bands, indicating homogeneity of the fold; the additional length of strands in the bimolecular construct results in retarded migration. Samples were prepared and electrophoresed on 20% non-denaturing PAGE as described in Experimental Section and were stained with EtBr. Appearance of a single band for each sample implies that each sample adopted a homogeneous fold. Migration was consistent with formation of the monomer for each unimolecular sample.

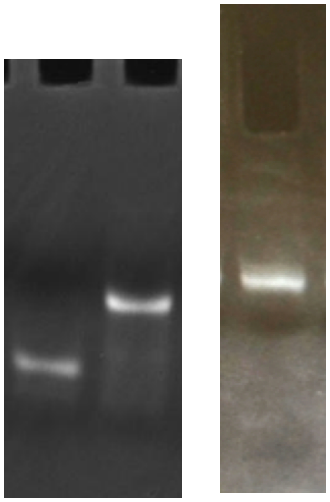

2A **2B**

Figure S-2B: Folding of the unimolecular sample *Arabidopsis* U12-U6$_{atac}$ snRNA complex (right; sequence above, and scheme of predicted fold in Fig. 2B).

Figure S-3: A 1D spectrum of imino protons of the bimolecular (top, Figure 1B) and unimolecular (bottom, Figure 2A) human U12-U6$_{atac}$ snRNA complex illustrates peaks of similar peak areas for the unimolecular construct, consistent with the anticipated number of hydrogen-bonded imino protons undergoing medium-slow exchange. Spectra acquired with mixing time 150 ms, 10 °C, at 600 MHz. The sample for both constructs was ~0.5 mM RNA in 10mM NaPi, 50 mM NaCl, 95% H_2O, 5% D_2O. Other acquisition parameters are in the Experimental Section.

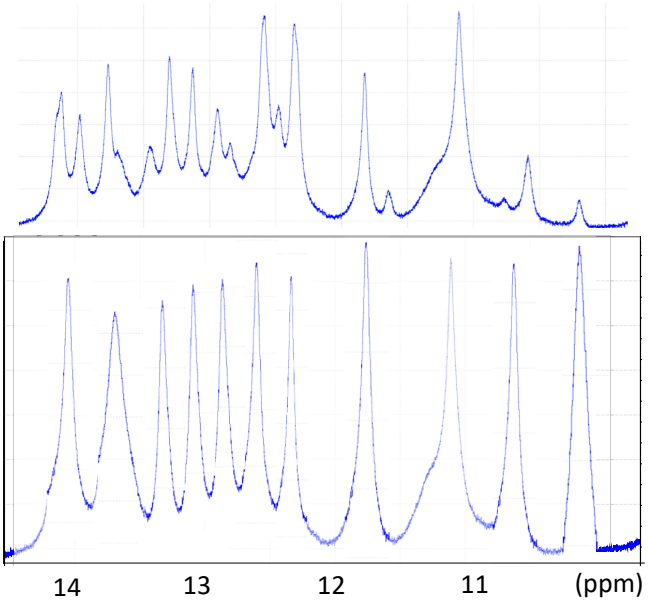

Figure S-4: Overlaying aromatic-anomeric (base-H1′) region of a 2D NOESY spectra for the bimolecular (Fig. 1B, red font) and unimolecular (Fig. 2A, black font) human U12-U6$_{atac}$ snRNA complex constructs indicate structural equivalence of the areas probed. The sample was ~0. 5 mM RNA in 10mM NaPi, 50 mM NaCl, in 99.996% D_2O. The spectrum was collected at 600 MHz, at 25 °C, with a mixing time 250 ms. Other acquisition parameters are in Experimental Section.

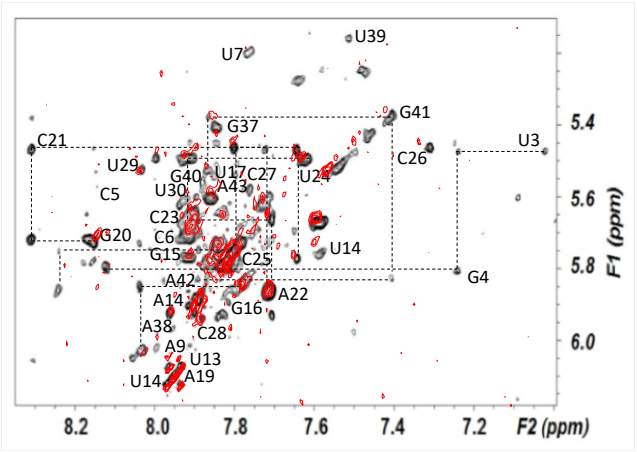

Figure S-5: 2D Aromatic-anomeric (base-H1′) region of a 2D NOESY spectrum of nonexchangeable protons used for analysis of sequential assignments. Nucleotides and connectivities identify base-H1′ nOes. The sample was ~0.5 mM RNA in 10mM NaPi, 50 mM NaCl, in 99.996% D_2O. The spectrum was collected at 600 MHz, at 25 °C, with a mixing time 250 ms. Other acquisition parameters are in Experimental Section.

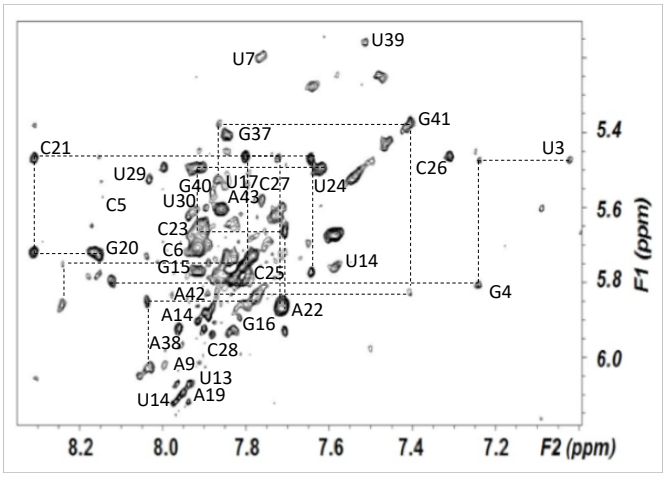

Figure S-6: Fluorescence assays to quantify affinity between human RBM22 and the human U12-$U6_{atac}$ snRNA complex (Figure 1B) were performed with by mixing 15-30 μM protein with RNA concentrations ranging from 3-42 μM so that each independent sample representing a molar ratio of 0.2:1 - 1.4:1 (RNA:protein) with an excitation at 300 nm and detection of emission at 350 nm. Further details are in Experimental Section. Samples highlighted here include (0.2:1, 0.6:1, 0.8:1, 1:1 for RNA:protein).

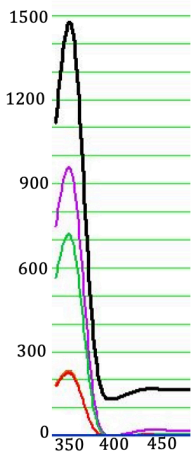

Figure S-7: Fluorescence assays to quantify affinity between human RBM22 and the human U2-U6 snRNA complex (Figure 1A) were performed with 15-30 μM RBM22 with RNA concentrations ranging from 3 μM-42 μM so that each independent sample representing a molar ratio of 0.2:1 - 1.4:1 (RNA:protein) with an excitation at 300 nm and detection of emission at 350 nm. Further details are in Experimental Section. Samples highlighted here include (0.2:1, 0.6:1, 0.8:1, 1:1 for RNA:protein).

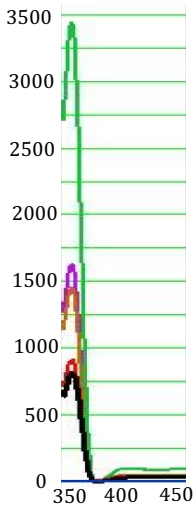

Figure S-8: Fluorescence assays for 30 μM RBM22 (left) and 30 μM RBM22 + 30 μM U5 snRNA, a non-binding RNA fragment, (right) with an excitation at 300 nm and detection of emission at 350 nm are highlighted here. This experiment serves as a control to correct for inner filter effects and provided identical results for both assays. Further details are in Experimental Section

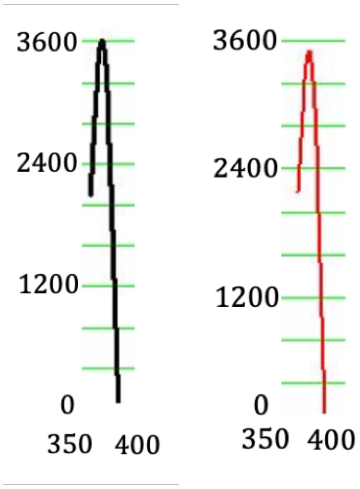

Table S-1: NMR Chemical shifts for ^{1}H and ^{15}N (imino) in the human U12-$U6_{atac}$ snRNA unimolecular construct (Fig. 2A in text). Shifts were derived from NMR experiments described the Experimental Section/Results in the text and were the same for corresponding nucleotides in the bimolecular construct (Fig. 1B in text).

Residue	H8/H6	H5/H2	H1′	H2′	H3′	H1/H3	^{15}N1/^{15}N3
U3	7.75	4.58	5.41	4.29	4.51	13.93	161
G4	7.82	-	5.86	4.71	4.47	12.2	143
C5	7.78	5.34	5.60	4.22	4.44	-	-
C6	8.03	5.84	5.71	4.31	4.37	-	-
U7	7.70	4.52	5.24	4.20	4.44	13.16	157
U8	7.82	4.99	5.48	4.41	4.35	12.81	158
A9	8.36	7.42	6.07	4.46	4.88	-	-
A10	8.24	7.35	5.98	4.40	4.80	-	-
A11	8.16	7.12	5.75	4.35	4.75	-	-
C12	8.07	5.86	5.74	4.28	4.32	-	-
U13	8.04	5.97	6.13	4.46	4.29	10.52	156
U14	8.00	5.90	6.10	4.38	4.25	13.96	161
A14	8.09	7.10	5.87	4.24	4.60	-	-
G15	7.13	-	5.76	4.64	4.57	11.22	142
G16	8.48	-	5.87	4.18	5.16	13.22	148
U17	7.85	4.68	5.56	4.35	4.57	14.21	163
U18	7.90	4.72	5.64	4.44	4.64	14.62	164
A19	8.32	7.38	6.11	4.44	4.85	-	-
G20	7.88	-	5.78	4.61	4.72	13.46	148
C21	7.48	5.29	5.40	4.51	4.60	-	-
A22	7.75	7.04	5.84	4.10	4.24	-	-
C23	7.84	5.33	5.65	4.25	4.30	-	-
U24	7.42	4.51	5.52	4.28	4.15	10.2	153
C25	7.67	5.23	5.74	4.45	4.47	-	-
C26	7.73	5.41	5.56	4.15	4.31	-	-
C27	7.69	5.31	5.58	4.21	4.45	-	-
C28	7.75	5.51	5.92	4.07	4.16	-	-
U29	7.83	4.64	5.52	4.36	4.22	13.5	162
U30	7.86	4.70	5.61	4.53	4.32	13.8	165
G31	7.76	-	5.88	4.39	4.69	12.43	146
A32	8.08	7.05	5.93	4.22	4.36	-	-
C33	7.82	5.62	5.51	4.31	4.53	-	-
A34	8.11	8.08	5.65	4.28	4.45	-	-
A35	8.20	7.30	5.84	4.38	4.64	-	-
G36	6.95	-	5.21	4.21	4.01	12.54	147
G37	6.82	-	5.32	4.25	4.08	12.73	149
A38	8.41	7.48	5.92	4.49	4.92	-	-
U39	7.64	4.17	5.21	4.28	4.16	13.16	151
G40	8.23	-	5.52	4.42	4.71	13.12	150
G41	6.89	-	5.45	4.32	4.29	11.62	140
A42	8.02	7.52	5.83	4.18	4.32	-	-
A43	7.98	7.01	5.68	4.16	4.28	-	-

Table S-2: NMR Chemical shifts for ^{1}H in the *Arabidopsis* U12-U6$_{atac}$ snRNA unimolecular construct (Fig. 2B in text) for select nucleotides in and surrounding the single-stranded hinge region of the ISL. Shifts were derived from NMR experiments described in Experimental Section/Results in the text.

Residue	H8/H6	H5/H2	H1′	H2′	H3′	H1/H3
G26	7.16	-	5.74	4.61	4.61	11.31
G27	8.45	-	5.86	4.22	5.18	12.46
C28	7.45	5.32	5.43	4.50	4.62	-
A29	7.73	7.01	5.86	4.12	4.21	-
U30	7.80	4.64	5.61	4.27	4.31	13.1
C31	7.72	5.36	5.61	4.28	4.31	-
U32	7.40	4.54	5.55	4.29	4.12	10.3
C33	7.65	5.25	5.51	4.44	4.48	-

Table S-3: Distances measured for inter-nucleotide steps for nucleotides in the ISL of single-stranded vs. double-stranded regions in the unimolecular human U12-U6$_{atac}$ snRNA complex. See Fig. 2A in the text for the construct and Experimental Section/Results for experimental details. For each dinucleotide step, interproton distances were measured for aromatic$_n$-aromatic$_{n+1}$ and anomeric$_n$-aromatic$_{n+1}$ distances.

single-stranded nucleotide step	H6/H8-H6/H8 distance (Å)	H1′-H6/H8 distance (Å)	double-stranded (control) nucleotide step	H6/H8-H6/H8 Distance (Å)	H1′-H6/H8 distance (Å)
A22-C23	4.7	4.8	A11-C12	3.2	3.4
C23-U24	4.5	4.7	CU12-U13/ C28-U29	3.0/ 3.1	3.3

Table S-4: Distances measured for inter-nucleotide steps for nucleotides in the ISL of single-stranded vs. double-stranded regions in the unimolecular *Arabidopsis* U12-$U6_{atac}$ snRNA complex. See Fig. 2B in the text for the construct and Experimental Section/Results for experimental details. For each dinucleotide step, interproton distances were measured for $aromatic_n$-$aromatic_{n+1}$ and $anomeric_n$-$aromatic_{n+1}$ distances.

single-stranded Nucleotide Step	H6/H8-H6/H8 distance (Å)	H1′-H6/H8 distance (Å)	double-stranded (control) nucleotide Step	H6/H8-H6/H8 distance (Å)	H1′-H6/H8 distance (Å)
C28-A29	4.6	4.8	C40-A41	3.2	3.5
A29-U30	4.3	4.6	A11-C12	3.3	3.6